Engineering Science and Technology, an International Journal 21 (2018) 778–786

HOSTED BY

ELSEVIER

Contents lists available at ScienceDirect

Engineering Science and Technology, an International Journal

journal homepage: www.elsevier.com/locate/jestch

Full Length Article

# Damped forced vibration analysis of single-walled carbon nanotubes resting on viscoelastic foundation in thermal environment using nonlocal strain gradient theory

Mohammad Malikan [a,*], Van Bac Nguyen [b], Francesco Tornabene [c]

[a] Department of Mechanical Engineering, Faculty of Engineering, Islamic Azad University, Mashhad Branch, Mashhad, Iran
[b] Department of Mechanical Engineering and the Built Environment, College of Engineering and Technology, University of Derby, Derbyshire, United Kingdom
[c] Department of Civil, Chemical, Environmental, and Materials Engineering, University of Bologna, Bologna, Italy

ARTICLE INFO

*Article history:*
Received 17 February 2018
Revised 17 May 2018
Accepted 1 June 2018
Available online 19 June 2018

*Keywords:*
Forced vibration
Single walled carbon nanotube
A new refined beam theory
Higher-order nonlocal strain gradient theory
Dynamic deflection

ABSTRACT

In this paper, the damped forced vibration of single-walled carbon nanotubes (SWCNTs) is analyzed using a new shear deformation beam theory. The SWCNTs are modeled as a flexible beam on the viscoelastic foundation embedded in the thermal environment and subjected to a transverse dynamic load. The equilibrium equations are formulated by the new shear deformation beam theory which is accompanied with higher-order nonlocal strain gradient theory where the influences of both stress nonlocality and strain gradient size-dependent effects are taken into account. In this new shear deformation beam theory, there is no need to use any shear correction factor and also the number of unknown variables is the only one that is similar to the Euler-Bernoulli beam hypothesis. The governing equations are solved by utilizing an analytical approach by which the maximum dynamic deflection has been obtained with simple boundary conditions. To validate the results of the new proposed beam theory, the results in terms of natural frequencies are compared with the results from an available well-known reference. The effects of nonlocal parameter, half-wave length, damper, temperature and material variations on the dynamic vibration of the nanotubes, are discussed in detail.


## 1. Introduction

Carbon nanotubes (CNTs) are allotropes of carbon with a cylindrical nanostructure; they are the first generation of the nano products that were discovered in 1991 [1]. The CNTs are made of twisted graphite sheets with a honeycomb-like structure. These nanotubes are very long and thin and also are stable, resistant, and flexible structures [2]. If the CNT only contains a pipe of graphene, it is called a single-walled carbon nanotube (SWCNT), and if it contains multiple rolled layers of graphene (concentric tubes), it is called a multi-wall carbon nanotube (MWCNT) [3,4]. The SWCNT is remarkably strong and hard [5], excellent in conducting electric current and directing heat [6–8], which has led to the wide use of these materials in the electronics industry, and one useful application is in the development of the first intermolecular field-effect transistors [9,10]. The MWCNT has many potential applications, from waterproof and tear resistant cloth fabrics, concrete and steel like applications based on the property of strength, electrical circuits based on the property of electrical conductivity, sensors based on the property of thermal conductivity, vacuum proof food packaging, and even as a vessel for delivering drugs. The carbon nanotube promises a bright future in cellular experiments because they can be used as nano-pipes to distribute very small volumes of fluid or gas into living cells or on surfaces [11–13].

These are nanostructures that are unique in their size, shape, and remarkable physical properties. To exploit the industrial amazing properties of such materials, it can be highly recommended that their mechanical behavior and properties should be investigated. In recent years, these intriguing mechanical properties have sparked much excitement and a large amount of studies by researchers around the world has been dedicated to their understanding. Malikan et al. [14] studied the nonlinear stability of bilayer graphene nanoplates subjected to shear and thermal forces in a medium using nonlocal elasticity theory and numerical solutions. In addition, Malikan investigated the stability of a micro sandwich plate with graphene coating using the refined couple

* Corresponding author.
*E-mail addresses:* mohammad.malikan@yahoo.com (M. Malikan), vb.nguyen@derby.ac.uk (V.B. Nguyen), francesco.tornabene@unibo.it (F. Tornabene).

Peer review under responsibility of Karabuk University.

https://doi.org/10.1016/j.jestch.2018.06.001
2215-0986/

stress theory [15] and buckling of graphene sheets subjected to nonuniform compression based on the four-variable plate theory using an analytical approach [16]. Yang et al. [17] examined the natural frequency of nonlinear free vibration of polymer composite beams reinforced with graphene nanoplatelets. Ansari et al. [18] studied coupled natural frequency analysis of post stability functionally graded micro/nanobeams on the basis of the strain gradient theory. Wang et al. [19] presented exact modes for post stability characteristics of nonlocal nanobeams in a longitudinal magnetic field. Analytical solutions for thermal vibration of nanobeams were studied by Jiang and Wang [20]; in this study, the Euler beam was modeled using nonlocal elasticity theory, and the beam was subjected to axial thermal forces. Xiang et al. [21] used nonlocal elasticity theory for studying nonlinear free vibration of double-walled carbon nanotubes based on Timoshenko beam theory. Li and Hu [22] presented buckling analysis of size-dependent nonlinear beams using nonlocal strain gradient theory. Guo et al. [23] developed a lower-order nonlocal strain gradient theory for evaluating vibration of nanobeams. The vibration of thermally post-buckled carbon nanotube-reinforced composite beams resting on elastic foundations was examined by Shen et al. [24]. Beni et al. [25] studied the vibration of shell nanotubes using nonlocal strain gradient theory and molecular dynamics simulation; in this study, a lower-order nonlocal strain gradient theory combining with first-order shear plate theory was adopted in order to obtain governing equations. Wang et al. [26] presented the nonlinear vibration of carbon nanotubes placed on the visco-Pasternak foundation under excitation frequency by nonlocal continuum theory. Chaudhari and Lal [27] investigated the nonlinear free vibration of elastically nanotubes reinforced composite beams resting on elastic foundation in thermal environment. They used higher-order shear deformation beam theory in conjunction with finite element models. The electro-mechanical vibration of single-walled nanotubes considering piezoelectric effects has been studied by Kheibari and Beni [28]. They modeled nanotubes as a thin shell model with the help of couple stress theory and then the governing equations were solved using Kantorovich method. Malekzadeh et al. [29] introduced a pre-twisted functionally graded (FG) carbon nanotube reinforced composite beam exposed to a vibrational condition based on the higher-order shear deformation theory of beams by considering the temperature dependence of material properties and the initial thermal stresses. The SWCNTs with several distributions reinforced the square FG-beam in thermal environment was considered and the Reddy's third-order shear deformation beam theory was employed to derive governing equations. Jiang et al. [30] analyzed the forced vibration of SWCNTs using molecular dynamics simulation based on one and three-segment Timoshenko beam models. Chang [31] studied the stochastic dynamics behavior of SWCNTs with random material properties resting on a nonlinear damper and subjected to an axial magnetic field without using any dynamics load. The nonlocal elasticity theory was applied to take small scale effects into consideration. The Monte Carlo simulation, Galerkin's and the multiple scale methods were utilized to predict the response of nonlinear governing equations which were derived from the Hamilton's principle. Jiang and Wang [32] studied the vibration of double-walled carbon nanotubes bridged on a silicon substrate and the nanotubes were modeled with Timoshenko beam model. Ren et al. [33] modeled nanotubes as functionally graded porous beams under free vibrational conditions. They used a two-variable refined beam theory combined with the nonlocal strain gradient theory to formulate size-dependent influences. Navier solution method was adopted to solve the frequency equation and the most significant results revealed that the presence of porosity could increase or decrease the natural frequency based on the grading index values. There have also been many valuable research in which carbon nanotubes have been investigated in several conditions [34–42].

In this theoretical work, a new shear deformation beam theory developed by reducing the unknown variables from a regenerated first-order shear deformation theory is used for the vibration analysis of a single-walled carbon nanotube. The single-walled carbon nanotube (SWCNT) is modeled as an elastic beam resting on a viscoelastic foundation in the thermal environment and subjected to a transverse dynamic harmonic load in order to evaluate excitation frequencies and thermo-vibrational behavior. Both stress nonlocality and strain gradient size-dependent influences are examined by using a higher-order nonlocal strain gradient theory. Furthermore, Navier's analytical approach is employed to solve the frequency equations by assuming simply-supported boundary conditions for both ends of the beam. The results obtained by the new theory are validated against the results available in literature.

## 2. Mathematical modeling

Fig. 1 displays a realistic model for a SWCNT resting on a viscoelastic foundation in a thermal environment subjected to the uniform transverse harmonic dynamic load. The tube has the length $L$, diameter $d$ and thickness $h$ parallel to $x$ and $z$-axes of the right-hand coordinate system, respectively.

Heretofore, many methods have been used for investigation of mechanical behavior of beams. The simplest theory for analysis of beams is the classical hypothesis which is based on Euler-Bernoulli's assumptions that the influences of transverse shear deformation are not taken into account. In this theory, it is assumed that during deformation, the cross section of the beam is to remain planar and normal to the deformed axis of the beam. This covered the case for small deflections of a beam that are subjected to lateral loads only and it is an appropriate theory to study thin beams (Euler-Bernoulli beam). However, due to the regardless of the shear and transverse strains along the thickness, using this beam theory is accompanied with errors in predicting the deformation or transient response of the beam in moderately thick and thick beams (Timoshenko's beam). In order to reduce this error in the analysis of relatively thick beams, another theory known as shear deformation one was introduced. In this theory, it is assumed that during deformation, there is a rotation between the cross section and the deformed axis of the beam as the transverse shear effects are taken into consideration. Although these shear deformation theories could produce reasonable results in the analysis of moderately thick beams, they are still not close to exact results due to the non-consideration of the effect of transverse strains ($\varepsilon_z = 0$). The first-order shear deformation theory is accompanied with a serious error for which the shear correction factor has been used. This means that the shear stress along the thickness of the beam is assumed to be constant, which is not realistic. To overcome this problem and to achieve the accuracy in predicting the beam behavior, a new first-order shear deformation beam theory has been introduced. According to the first-order shear deformation theory, the displacement field at any material point in the beam could be defined as follows [14]:

$$\begin{Bmatrix} U(x,z,t) \\ V(x,z,t) \\ W(x,z,t) \end{Bmatrix} = \begin{Bmatrix} u(x,t) + z\varphi(x,t) \\ 0 \\ w(x,t) \end{Bmatrix} \tag{1a-c}$$

In Eq. (1), the vector quantities of the neutral axis at directions of $x$ and $z$ are $u$ and $w$, respectively. Furthermore, for defining of the swirl of beam elements around the $x$ axis, $\varphi$ is used. First of all, the simple first-order shear deformation theory (S-FSDT) is recalled where the deflection parameter could be expressed as follows [43–45]:

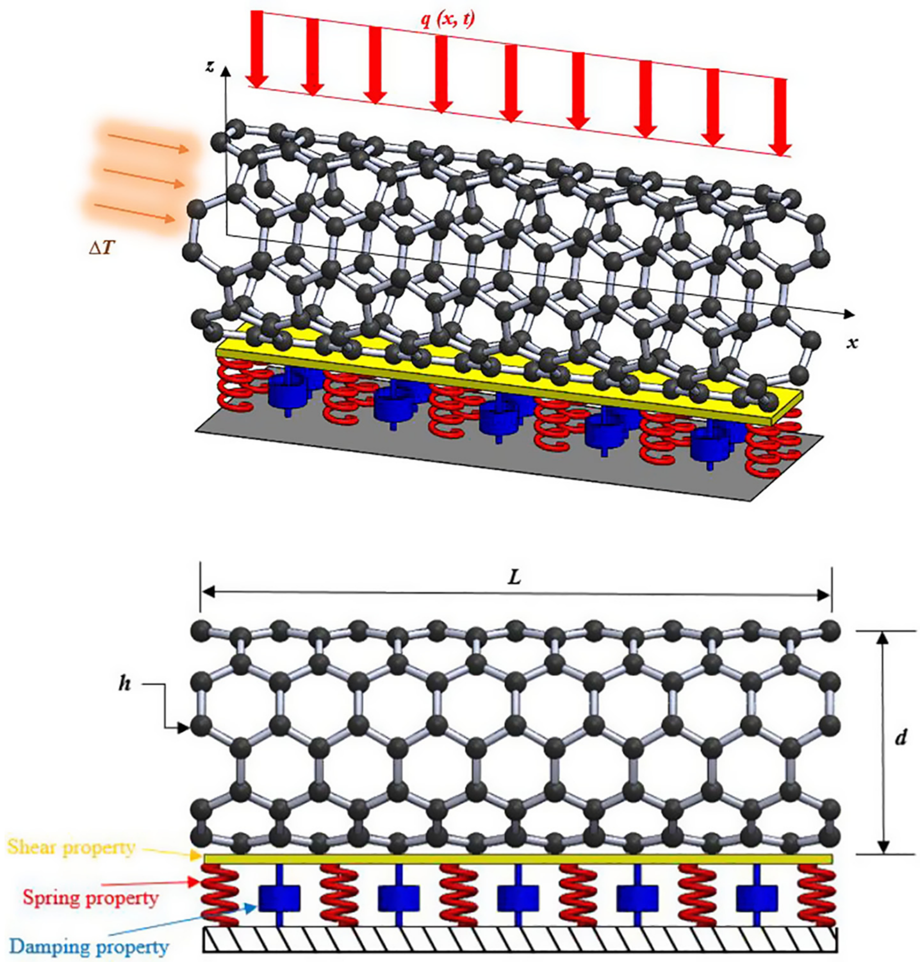


**Fig. 1.** Schematic representation of the single-walled carbon nanotube resting on the viscoelastic matrix in a thermal environment and subjected to a transverse harmonic load).



$$w = w(bending) + w(shear) \tag{2}$$

On the other hand, the rotation parameter was developed as follows:

$$\{\phi\} = \left\{-\frac{\partial w_b}{\partial x}\right\} \tag{3}$$

Substituting the parameters in Eqs. (2) and (3) into Eq. (1) the displacement field of the simple first-order shear deformation theory is rewritten [15,16,43–45]:

$$\begin{Bmatrix} U(x,z,t) \\ W(x,z,t) \end{Bmatrix} = \begin{Bmatrix} u(x,t) - z\frac{\partial w_b(x,t)}{\partial x} \\ w_b(x,t) + w_s(x,t) \end{Bmatrix} \tag{4a-b}$$

Expressing $w = w_b + w_s$ might not be conceptual; therefore, the S-FSDT could be refined in the following equations:

$$\begin{Bmatrix} U(x,z,t) \\ W(x,z,t) \end{Bmatrix} = \begin{Bmatrix} u(x,t) - z\frac{\partial w_b(x,t)}{\partial x} \\ w_b(x,t) + W' \end{Bmatrix} \tag{5a-b}$$

So, the bending deflection could be used to find the value of $w_s$:

$$\begin{Bmatrix} \sigma_{xx} \\ \sigma_{xz} \end{Bmatrix} = \begin{Bmatrix} E\varepsilon_{xx} \\ 2G\gamma_{xz} \end{Bmatrix} \tag{6a-b}$$

After calculating Eq. (6) from Eq. (4), the stresses could be harvested, and then by substituting Eq. (6) into Eq. (7) the S-FSDT stress resultants could now be presented as follows:

$$\begin{Bmatrix} M_{xx} \\ Q_x \end{Bmatrix} = \int_A \begin{Bmatrix} \sigma_x z \\ \sigma_{xz} \end{Bmatrix} dA \tag{7a-b}$$

The fourth equation of FSDT's governing equations could be used in order to obtain $w_s$ from $w_b$:

$$\frac{\partial M_x}{\partial x} - Q_x = 0 \tag{8}$$

Now by imposing Eq. (8) into the stress resultants of Eq. (7):

$$EI_c\frac{\partial^3 w_b}{\partial x^3} - AG\frac{\partial w_s}{\partial x} = 0 \tag{9}$$

By integrating Eq. (9) with respect to $x$ and then simplifying, the shear deflection could now be obtained as follows:

$$w_s = W' = B\frac{\partial^2 w_b}{\partial x^2} \tag{10}$$

Term $B$ is explained below:

$$B = \frac{EI_c}{AG}, \quad G = \frac{E}{2(1+\upsilon)} \tag{11}$$

where $G$ represents the shear modulus, $E$ is the Young's modulus, $I_c$ ($I_c = \int_A z^2 dA$) denotes the moment of area of the cross-section, $A$ is the cross-sectional area and $v$ is the Poisson's ratio for isotropic nanobeams. Eventually, the new beam theory could be achieved as:

$$\text{Now}: w_b = w_0; \begin{Bmatrix} U(x,z,t) \\ W(x,z,t) \end{Bmatrix} = \begin{Bmatrix} u(x,t) - z\dfrac{\partial w_0(x,t)}{\partial x} \\ w_0(x,t) + B\dfrac{\partial^2 w_0(x,t)}{\partial x^2} \end{Bmatrix} \tag{12a-b}$$

Using Hamilton's principle, the potential energy in the whole domain of the beam ($V$) was made available and is written in the variational form as follows [20,46]:

$$\delta V = \delta \int_0^t (S + \Omega - T)dt = 0 \tag{13}$$

In which $\delta S$ is the variation of strain energy, and for the variation of kinetic energy $\delta T$ has been allocated and $\delta V$ is the variation of works, which are done by external forces. The strain energy by variational formulation could be calculated:

$$\delta S = \int\int_v \int \sigma_{ij}\delta\varepsilon_{ij} dV = 0 \tag{14}$$

The strain tensor in Eq. (14) is expanded as follows:

$$\begin{Bmatrix} \varepsilon_{xx} \\ \gamma_{xz} \end{Bmatrix} = \begin{Bmatrix} \dfrac{\partial u}{\partial x} - z\dfrac{\partial^2 w_0}{\partial x^2} + \dfrac{1}{2}\left(B\dfrac{\partial^3 w_0}{\partial x^3} + \dfrac{\partial w_0}{\partial x}\right)^2 \\ B\dfrac{\partial^3 w_0}{\partial x^3} \end{Bmatrix} - \begin{Bmatrix} \alpha\Delta T \\ 0 \end{Bmatrix} \tag{15a-b}$$

In which $\alpha$ is the thermal expansion coefficient and $\Delta T$ is the thermal changes across the thickness of the nanobeam ($\Delta T = T_2 - T_1$, $T_1$ = *300 K-room temperature*). The kinetic energy of the beam could be calculated as [20,46]:

$$T = \frac{1}{2}\rho \int\int_A \left(\left(\frac{\partial U}{\partial t}\right)^2 + \left(\frac{\partial W}{\partial t}\right)^2\right) dAdx = 0 \tag{16}$$

So the kinetic energy in the variational form could be expanded in the following form:

$$\delta T = \rho \int\int_A \left(-z^2\frac{\partial^4 w_0}{\partial x^2\partial t^2} - \frac{\partial^2 w_0}{\partial t^2} - B^2\frac{\partial^6 w_0}{\partial x^4\partial t^2} - 2B\frac{\partial^4 w_0}{\partial x^2\partial t^2}\right)\delta w_0 dAdx = 0 \tag{17}$$

In which $\rho$, $m_0$ ($m_0 = \rho\int_A dA$), and $I_m$ ($I_m = \rho I_c$) are the volumetric mass density, sectional density and mass moment of inertia, respectively. With applying the variational formulation ($\delta V = 0$) the nonlinear governing equation of motion is derived as follows:

$$\begin{aligned} \delta w_0 = 0; \quad & -\frac{\partial^2 M_x}{\partial x^2} + B\frac{\partial^3 Q_x}{\partial x^3} + N_x\left(B^2\frac{\partial^6 w_0}{\partial x^6} + \frac{\partial^2 w_0}{\partial x^2} + 2B\frac{\partial^4 w_0}{\partial x^4}\right) \\ & - I_m\left(\frac{\partial^4 w_0}{\partial x^2\partial t^2}\right) - m_0\left(\frac{\partial^2 w_0}{\partial t^2} + B^2\frac{\partial^6 w_0}{\partial x^4\partial t^2} + 2B\frac{\partial^4 w_0}{\partial x^2\partial t^2}\right) = q(x,t) \end{aligned} \tag{18}$$

In which $M_x$, $Q_x$, and $N_x$ are nonlocal stress resultants, respectively. Here, the quantity $N_x$ is the resultant with respect to the axial applied in-plane force. According to the higher-order nonlocal strain gradient theory, the following equation is employed [47–50]:

$$\begin{aligned} (1-\mu_1^2\nabla^2)(1-\mu_0^2\nabla^2)\sigma_{ij} &= \mathrm{C}_{ijkl}(1-\mu_1^2\nabla^2)\varepsilon_{kl} \\ &\quad - \mathrm{C}_{ijkl}l^2(1-\mu_0^2\nabla^2)\nabla^2\varepsilon_{kl}; \\ \mu_0(nm) = e_0 a, \ \mu_1(nm) &= e_1 a, \ \nabla^2 = \frac{\partial^2}{\partial x^2} \end{aligned} \tag{19}$$

where $\mu_0$, $\mu_1$, and $l$ are lower and higher-order nonlocality factors and strain gradient length scale characteristic, respectively. Furthermore, $a$ is an interior determined length. The Eq. (19) could be easily converted into other forms of nonlocal theory as follows:

Lower-order nonlocal strain gradient theory:

$$\begin{Bmatrix} \mu_0 = e_0 a \\ \mu_1 = e_1 a \end{Bmatrix} \to \mu_0 = \mu_1 = \mu \to (1-\mu^2\nabla^2)\sigma_{ij} = C_{ijkl}(1-l^2\nabla^2)\varepsilon_{kl} \tag{20}$$

a) Eringen's nonlocal elasticity theory:

$$\{l = \mu_1 = 0 \to (1-\mu_0^2\nabla^2)\sigma_{ij} = C_{ijkl}\varepsilon_{kl} \tag{21}$$

b) A model without stress nonlocality:

$$\{\mu_0 = \mu_1 = 0 \to \sigma_{ij} = \mathrm{C}_{ijkl}(1-l^2\nabla^2)\varepsilon_{kl} \tag{22}$$

By using higher-order nonlocal strain gradient theory and applying it on the stress resultants, the following equation is obtained:

$$\begin{aligned} (1-\mu_1^2\nabla^2)(1-\mu_0^2\nabla^2)\sigma_{ij} &= \mathrm{C}_{ijkl}(1-\mu_1^2\nabla^2)\varepsilon_{kl} \\ &\quad - \mathrm{C}_{ijkl}l^2(1-\mu_0^2\nabla^2)\nabla^2\varepsilon_{kl} \end{aligned} \tag{23}$$

The stress resultants in local form are specified by relations below:

$$\begin{Bmatrix} M_x \\ Q_x \end{Bmatrix} = \int_A \begin{Bmatrix} \sigma_x z \\ \sigma_{xz} \end{Bmatrix} dA \tag{24a-b}$$

Now, substituting Eq. (15) into the Eq. (24) the stress resultants could be expressed as follows:

$$\begin{Bmatrix} \mathrm{M_x} \\ \mathrm{Q_x} \end{Bmatrix} = \begin{Bmatrix} -EI_c\frac{\partial^2 w_0}{\partial x^2} \\ AGB\frac{\partial^3 w_0}{\partial x^3} \end{Bmatrix} \tag{25a-b}$$

The in-plane thermal force which is obtained from the axial thermal strain as follows:

$$N^0 = -N^T = -EA\alpha\Delta T \tag{26}$$

Then, the Eq. (23) is used to rewrite the stress resultants in higher-order nonlocal forms:

$$\begin{aligned} &\left(1-(\mu_0^2+\mu_1^2)\nabla^2 + \mu_0^2\mu_1^2\nabla^4\right) \\ &M_x = -\left[(1-\mu_1^2\nabla^2) - l^2(1-\mu_0^2\nabla^2)\nabla^2\right]\left(EI_c\frac{\partial^2 w_0}{\partial x^2}\right) \end{aligned} \tag{27a}$$

$$\begin{aligned} &\left(1-(\mu_0^2+\mu_1^2)\nabla^2 + \mu_0^2\mu_1^2\nabla^4\right)Q_x \\ &= \left[(1-\mu_1^2\nabla^2) - l^2(1-\mu_0^2\nabla^2)\nabla^2\right]AG\left(B\frac{\partial^3 w_0}{\partial x^3}\right) \end{aligned} \tag{27b}$$

Now, by incorporating Eq. (27) and using Eq. (26) and inserting them into Eq. (18), the thermal forced vibration equation could be acquired.

When the mechanical behavior of nanobeams is studied, the beam could be deployed on a base as an impressive stability factor. In this paper, the Pasternak elastic foundation was initially used but by examining the vibrational problem, the viscous matrix was later added to the Pasternak medium in order to take into account the damper effects for the foundation. Indeed, the effect of damping should be considered in the foundation whilst the beam was undergoing dynamic loads. For this purpose, the Visco-Pasternak foundation was introduced as an external force which is defined as follows [46]:

$$V = \int_0^L \left(k_G\nabla^2 w_0 - k_w w_0 - C_d\frac{\partial w_0}{\partial t}\right)\delta w_0 dx \tag{28}$$

In which $k_G$, $k_w$, and $C_d$ are shear modulus, stiffness modulus and damper coefficient in the viscoelastic matrix, respectively.

## 3. Analytical approach

In order to apply the simple boundary condition and solve the stability equation, the Navier's solution is employed. Using this method, the displacement field and potential functions could be expanded in the following form [50]:

$$\mathrm{w}_0(x,t) = \sum_{m=1}^{\infty} \mathrm{W}_{\mathrm{m}} \exp(i\omega_n t) \sin\left(\frac{m\pi}{L}x\right), \quad i = \sqrt{-1} \tag{29}$$

In which $W_{0mn}$ is the displacement quantity, $m$ is the half-wave number and $\omega_n$ denotes the natural frequency related to intrinsic properties of the system such as mass and stiffness. In this paper, it is assumed that the dynamic load was distributed uniformly and acted harmonically (Fig. 1); that could be taken in the form of the following expression [51]:

$$q(x,t) = \sum_{m=1}^{\infty} q_m \exp(i\omega_{ex} t) \sin\left(\frac{m\pi}{L}x\right) \tag{30a}$$

$$\begin{aligned} q_m &= \frac{2}{L}\int_{x_0-c/2}^{x_0+c/2} q_0 \sin\left(\frac{m\pi}{L}x\right)dx \\ &= \frac{4q_0}{m\pi}\sin\left(\frac{m\pi}{L}x_0\right)\sin\left(\frac{m\pi}{L}\frac{c}{2}\right) \end{aligned} \tag{30b}$$

In which $q_m$ is the Fourier coefficient, $q_0$ is the uniform load amplitude, $x_0$ is the centroid of the uniform load, $c$ is the length of the distributed load and $\omega_{ex}$ is the excitation frequency, respectively.

Substituting Eq. (30) into the equation of motion, the algebraic equation is obtained as:

$$\begin{aligned} (K + C\Delta r + \Delta r^2 M)\{W_m\} = \{(1 - (\mu_0^2 + \mu_1^2)\nabla^2 \\ + \mu_0^2\mu_1^2\nabla^4)q(x,t)\} \end{aligned} \tag{31}$$

where $\Delta r = \omega_{ex}/\omega_n$ is the excitation to natural frequency ratio.

For convenience, the following parameters are used in order to obtain a non-dimensional equation.

$$\begin{aligned} &W = \frac{w_0}{L}, \eta = \frac{x}{L}, \quad \Gamma_0 = \frac{\mu_0}{L^2}, \quad \Gamma_1 = \frac{\mu_1}{L^2}, \quad l^* = \frac{l}{h}, \\ &Q = \frac{q_0}{EL}, \quad \mathrm{G}^* = \frac{G}{E}, \quad M_0 = \frac{m_0}{\rho L^2}, \quad \mathrm{I}_M = \frac{\mathrm{I}_m}{\rho L^4}, \quad \mathrm{B}^* = \frac{B}{L^3} \\ &\Omega = \omega L\sqrt{\frac{\rho}{E}}, \quad \mathrm{C_D} = \frac{C_d}{h\sqrt{\rho E}}, \quad \zeta = \frac{h}{L}, \quad \mathrm{I}_C = \frac{\mathrm{I}_c}{L^4}, \\ &\mathrm{A}^* = \frac{A}{L^2}, \quad \mathrm{K_W} = \frac{\mathrm{k}_w}{E}, \quad \mathrm{K}_G = \frac{\mathrm{k}_G}{EL^2}, \quad N^* = \frac{N^0}{EL^2} \end{aligned} \tag{32}$$

In which $K$ represents the dimensionless stiffness matrix, $C$ and $M$ are the dimensionless damping and mass matrixes. They are extracted in the following forms, respectively:

$$\begin{aligned} K = \Bigg\{ &\left(I_C\frac{\partial^4 W}{\partial\eta^4} + A^*G^*B^*\frac{\partial^6 W}{\partial\eta^6}\right) - (\Gamma_1^2 + l^{2*}\zeta^2)\left(I_C\frac{\partial^6 W}{\partial\eta^6} + A^*G^*B^*\frac{\partial^8 W}{\partial\eta^8}\right) \\ &+ l^{2*}\zeta^2\Gamma_0^2 \times \left(I_C\frac{\partial^8 W}{\partial\eta^8} + A^*G^*B^*\frac{\partial^{10} W}{\partial\eta^{10}}\right) \\ &+ N^*\left(\left(\frac{I_C^2}{A^{2*}G^{2*}}\right)\frac{\partial^6 W}{\partial\eta^6} + \frac{\partial^2 W}{\partial\eta^2} + 2\frac{I_C}{A^*G^*}\frac{\partial^4 W}{\partial\eta^4}\right) \\ &- N^*(\Gamma_0^2 + \Gamma_1^2) \times \left(\left(\frac{I_C^2}{A^{2*}G^{2*}}\right)\frac{\partial^8 W}{\partial\eta^8} + \frac{\partial^4 W}{\partial\eta^4} + 2\frac{I_C}{A^*G^*}\frac{\partial^6 W}{\partial\eta^6}\right) \\ &+ N^*\Gamma_0^2\Gamma_1^2\left(\left(\frac{I_C^2}{A^{2*}G^{2*}}\right)\frac{\partial^{10} W}{\partial\eta^{10}} + \frac{\partial^6 W}{\partial\eta^6} + 2\frac{I_C}{A^*G^*}\frac{\partial^8 W}{\partial\eta^8}\right) \\ &+ \left(\mathrm{K}_G\frac{\partial^2 W}{\partial\eta^2} - \mathrm{K_W}W\right) - (\Gamma_0^2 + \Gamma_1^2)\left(\mathrm{K}_G\frac{\partial^4 W}{\partial\eta^4} - \mathrm{K_W}\frac{\partial^2 W}{\partial\eta^2}\right) \\ &+ \Gamma_0^2\Gamma_1^2\left(\mathrm{K}_G\frac{\partial^6 W}{\partial\eta^6} - \mathrm{K_W}\frac{\partial^4 W}{\partial\eta^4}\right)\Bigg\} \end{aligned} \tag{33a}$$

$$C = -i\mathrm{C_D}\zeta\Omega\left\{W - (\Gamma_0^2 + \Gamma_1^2)\frac{\partial^2 W}{\partial\eta^2} + \Gamma_0^2\Gamma_1^2\frac{\partial^4 W}{\partial\eta^4}\right\} \tag{33b}$$

$$\begin{aligned} M = -\Omega^2\Bigg\{ &-\mathrm{I}_M\frac{\partial^2 W}{\partial\eta^2} - M_0\left(W + \frac{I_C^2}{A^{2*}G^{2*}}\frac{\partial^4 W}{\partial\eta^4} + 2\frac{I_C}{A^*G^*}\frac{\partial^2 W}{\partial\eta^2}\right) \\ &-(\Gamma_0^2 + \Gamma_1^2)\left(-\mathrm{I}_M\frac{\partial^4 W}{\partial\eta^4} - M_0\left(\frac{\partial^2 W}{\partial\eta^2} + \frac{I_C^2}{A^{2*}G^{2*}}\frac{\partial^6 W}{\partial\eta^6} + 2\frac{I_C}{A^*G^*}\frac{\partial^4 W}{\partial\eta^4}\right)\right) \\ &+\Gamma_0^2\Gamma_1^2\left(-\mathrm{I}_M\frac{\partial^6 W}{\partial\eta^6} - M_0\left(\frac{\partial^4 W}{\partial\eta^4} + \frac{I_C^2}{A^{2*}G^{2*}}\frac{\partial^8 W}{\partial\eta^8} + 2\frac{I_C}{A^*G^*}\frac{\partial^6 W}{\partial\eta^6}\right)\right)\Bigg\} \end{aligned} \tag{33c}$$

To obtain the natural frequencies, Eq. (31) could be solved by ignoring the transverse load. After calculating natural frequencies, the linear algebraic equation of motion could be solved in order to compute maximum dynamic deflections.

## 4. Numerical results and discussions

In this section, the vibration of single-walled carbon nanotubes (SWCNT) based on the new refined beam theory proposed in this paper is investigated. First of all, the accuracy of the numerical results originated from the one variable first-order shear deformation theory (OVFSDT) had to be compared and validated against other theories. In particular, it is very important to understand the differences generated in the results obtained by different theories. Therefore, Table 1 presents natural frequencies collated from the previous well-known research [25] and these are compared with results obtained by the present new refined beam theories combining with lower-order nonlocal strain gradient theory, or strain gradient theory, or nonlocal elasticity theory. In this table, the carbon nanotube (CNT) was modeled using the shell model and constitutive equations were derived on the basis of the FSDT; these were solved by using Navier's solution method and also employing molecular dynamics simulation (MD) for simple boundary conditions. Several cases of using different strain theories including lower-order nonlocal strain gradient theory, strain gradient theory and nonlocal strain theory are compared with the previous study's results [25] from which the accuracy of the present theories' outcomes could be approved. It can be seen clearly that using the strain gradient theory ($\mu_0 = 0$, $\mu_1 = 0$, $l \neq 0$) could not gain appropriate results for analyzing vibrations of mechanical systems, especially for small length ratios L/D. Increasing length of the CNT, the results of the nonlocal elasticity case ($\mu_0 \neq 0$, $\mu_1 = 0$, $l = 0$) became closer to MD-armchair CNT results; however, the results of the lower-order nonlocal strain gradient case are in a better agreement with the MD results. The difference among the results of OVFSDT when compared with the previous study's results [25] could be due to many conditions such as using shear correction factor in the FSDT, and/or modeling the CNT as a shell in this reference. Although modeling the CNT as a cylindrical shell might be more accurate than modeling it as a beam, solving the governing equations could be very expensive in terms of computational costs and time consuming. Therefore, modeling the CNT as a beam could be acceptable as reasonable results shown in the comparison section. Overall, it deemed that Table 1 shows excellent agreements in numerical results between the present theory's and others, indicating that the new refined theory could be used for analyzing the vibration of single-walled carbon nanotubes. Table 2 shows material properties of the CNT used in this study.

Fig. 2 shows the influences of the higher and lower-order nonlocal parameters on the dimensionless maximum dynamic deflections. Fig. 2a illustrates the influences on the results which are obtained for both the damped and undamped cases. It can be seen

**Table 1**
Comparison of natural frequencies (THz) obtained from different theories for the CNT. *E = 1.06TPa, υ = 0.19, $k_s$ = 5/6, h = 0.34 nm, d = 0.68 nm, CNT's shell model, SS* [25] *E = 1.06TPa, υ = 0.19, h = 0.34 nm, d = 0.68 nm, CNT's beam model, SS [Present theory] $e_0a$ = 3.3–3.5 nm, l = 0.1–0.4 nm [25-Present theory].*

| L/D | [25] (MD-armchair CNT) | Lower-order nonlocal strain gradient theory | | Strain gradient theory | | Nonlocal elasticity theory | |
|---|---|---|---|---|---|---|---|
| | | [25] (FSDT, Navier) | Present (OVFSDT, Navier) | [25] (FSDT, Navier) | Present (OVFSDT, Navier) | [25] (FSDT, Navier) | Present (OVFSDT, Navier) |
| 4.86 | 1.138 | 1.209 | 1.25535 | 12.42 | 12.35233 | 0.758 | 0.75967 |
| 8.47 | 0.466 | 0.448 | 0.43207 | 4.461 | 4.69543 | 0.333 | 0.35485 |
| 13.89 | 0.190 | 0.192 | 0.19004 | 1.957 | 1.98552 | 0.165 | 0.16355 |
| 17.47 | 0.122 | 0.126 | 0.12431 | 1.321 | 1.22947 | 0.121 | 0.12460 |

**Table 2**
Mechanical properties of the nanobeam [25,52–56].

| | |
|---|---|
| SWCNT | Elastic properties<br>*E = 1.06 TPa, ν = 0.19*<br>Other quantities<br>*h = 0.34 nm, d = 0.7 nm, L = 40d ρ = 2300 kg/m³, α = 1.1e−6 K⁻¹* |

clearly that when the value of the higher-order nonlocal parameter increases, the deflections decrease. This downward trend for the greater load is shown with a steeper slope. Furthermore, it is witnessed that for large values of the higher-order nonlocal parameter, the impact of the damper on the deflection is drastically decreased, and results for both cases are matched to each other. To complete the above discussion, the influences of different values of lower-order nonlocal parameter and half-waves on the deflection were investigated and results are shown in Fig. 2b. According to this figure, it is clear that the half-waves have strong effects on the deflection, and in the first half-wave, the gap between both cases are more noticeable.

Fig. 3 reveals the effects of frequency ratio on the dynamic deflection by taking various damping conditions. Fig. 3a presents the appropriate amount of the viscous damper in order to damp out the amplitude of the vibrations. As shown in the figure, when the damping is reduced, the dynamic deflection increased; the same phenomenon is observed when the frequency ratio increased. When the damper is removed and the frequency ratio increased, the dynamic deflection reached maximum values and it approached the resonance region ($\Delta r$ = 1). With the presence

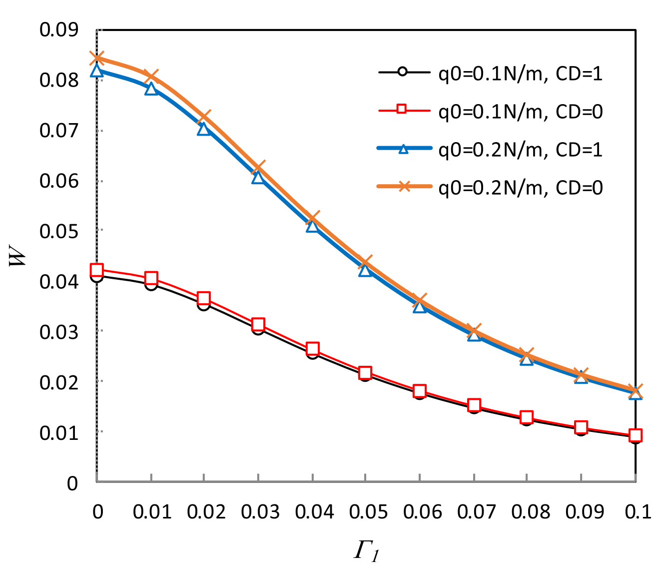


**Fig. 2a.** The higher-order nonlocal parameter versus the two damped and undamped cases ($\Gamma_0$ = 0.01, $l^*$ = 2, m = 3, $\Delta r$ = 0.1, $N^*$ = 0.001, $x_0$ = 0.5L, c = L, $K_W$ = 0.01, $K_G$ = 0.01).

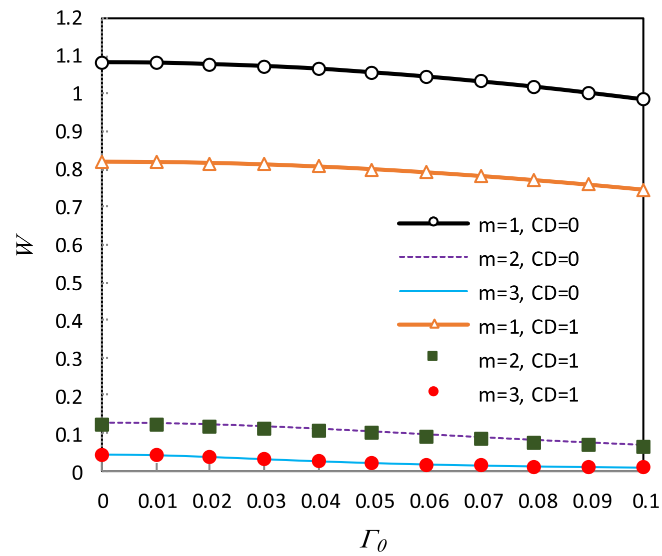


**Fig. 2b.** The lower-order nonlocal parameter versus different half-waves ($\Gamma_1$ = 0.01, $l^*$ = 2, $\Delta r$ = 0.1, $x_0$ = 0.5L, c = L, $K_W$ = 0.01, $K_G$ = 0.01, $q_0$ = 0.1 N/m, $N^*$ = 0.001).

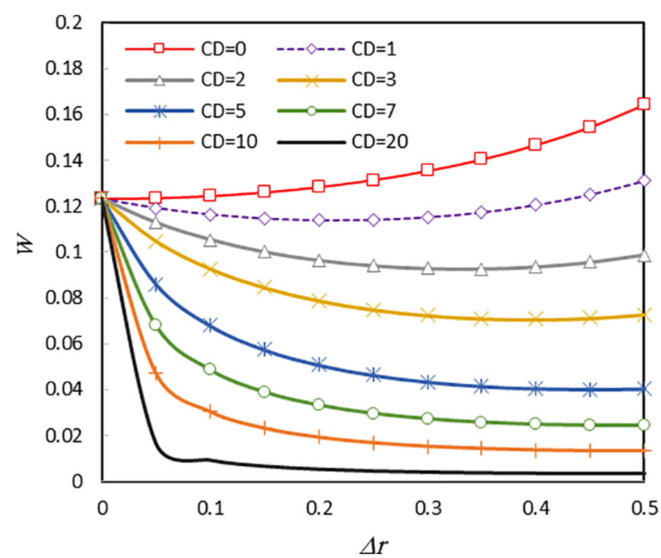


**Fig. 3a.** Frequency ratio versus various viscous damper quantities ($\Gamma_0$ = 0.01, $\Gamma_1$ = 0.02, $l^*$ = 2, m = 2, $q_0$ = 0.1 N/m, $x_0$ = 0.5L, c = L, $K_W$ = 0.01, $K_G$ = 0.01, $C_D$ = 1, $N^*$ = 0.001).

of the damper, the outcomes are reversed and whenever the dashpot is stronger the damping rate is higher, leading to an overdamping case. In fact, after the value $C_D$ = 3, the vibration went into a complete damping and with the frequency ratio about $\Delta r$ = 0.3, it is clear that the vibrating system subjected to the applied dynamic

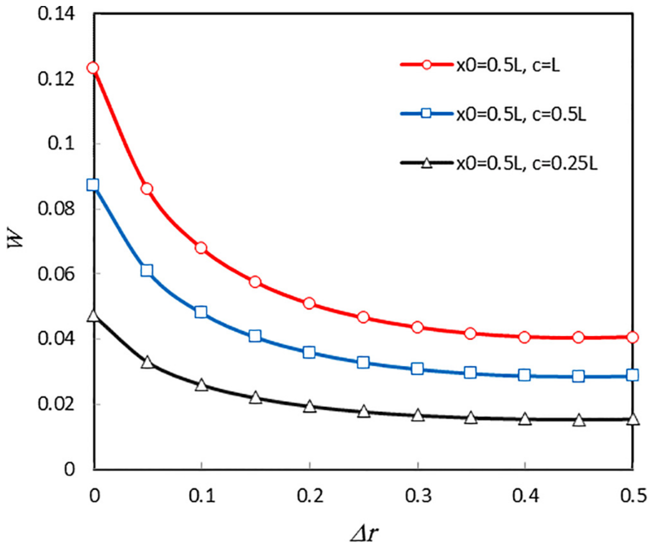


**Fig. 3b.** Frequency ratio versus different distributed loads ($\Gamma_0$ = 0.01, $\Gamma_1$ = 0.02, $l^*$ = 2, m = 2, $q_0$ = 0.1 N/m, $K_W$ = 0.01, $K_G$ = 0.01, $C_D$ = 5, $N^*$ = 0.001).

load is entirely damped out; and the negative effects of vibrations are eliminated. As a matter of fact, if the deflection is expressed based on time, the period that the number of cycles taken for damping to be completed, could be obtained. On the other hand, Fig. 3b illustrates the distribution of harmonic load on the nanobeam at various damping conditions. It is worth noting that when the load distribution became smaller, the maximum deflection increased accordingly.

The influences of the in-plane force resultants obtained from the change of temperature (in the thermal environment) versus several higher and lower-order nonlocal dimensionless parameters are demonstrated in Fig. 4. It can be seen that in the case $\Gamma_0 = 0.01$, $\Gamma_1 = 0.01$, which is the general nonlocal strain gradient case, the dynamic deflections reached largest values. This means that when the higher-order nonlocal strain gradient conditions ($\Gamma_0 \neq \Gamma_1$) is considered, the outcomes of the proposed theory are lower than the previous conditions. It can also be seen that in terms of changing the heat in the environment, increasing the temperature increased significantly the difference between the results of the higher and lower-order nonlocal cases. The difference had an increasing trend which shows the importance of the use of higher-order nonlocal strain gradient case at high temperatures.

Fig. 5 presents the influences of different parameters of the foundation versus higher and lower-order nonlocal cases. In Fig. 5a, the variations of the stiffness modulus of the elastic foundation show that when the stiffness increased, the deflections are reduced. With regard to the negative slope of the curves W-$K_W$, as a rule, if the stiffness of the matrix approaches infinity, the dynamic deflection reaches zeros. Fig. 5b shows the shear effect of the elastic medium on the deflection, in which the curves W-$K_G$ are nonlinear and this is different to the curves in Fig. 5a in which the curves were linear. In other words, the decreasing effects of results are more noticeable in the shear modulus than the stiffness modulus, which could prove that the results of shear layer are more unpredictable than the stiffness factor on the outcomes of the forced vibrational system. The notable point could be that with an increase in shear factor magnitudes, the results of the three nonlocal cases are approaching to each other's, and

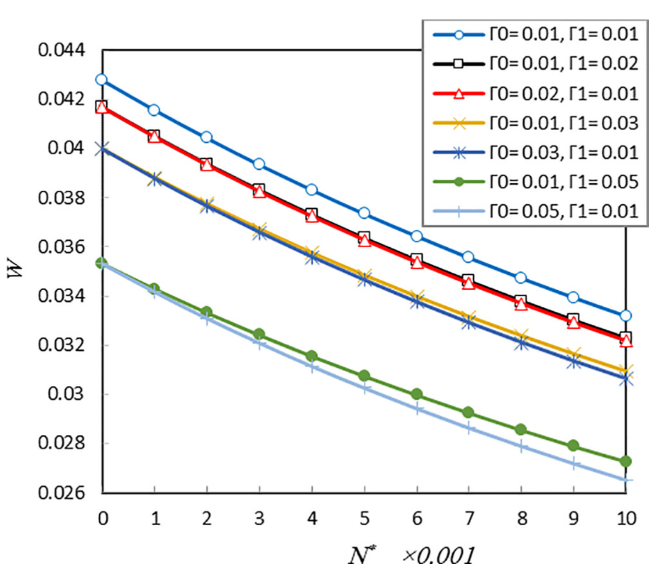


**Fig. 4.** Temperature changes versus higher and lower-order nonlocal parameters ($l^*$ = 2, m = 2, Δr = 0.5, $q_0$ = 0.1 N/m, $x_0$ = 0.5L, c = L, $K_W$ = 0.01, $K_G$ = 0.01, $C_D$ = 5).

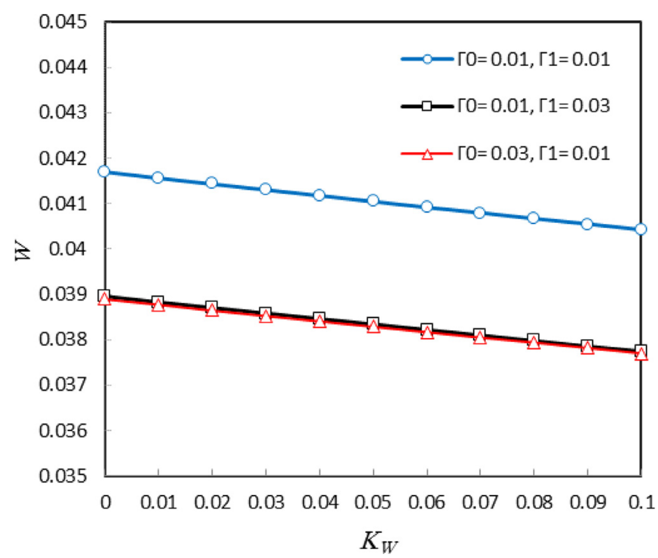


**Fig. 5a.** Stiffness modulus versus higher and lower-order nonlocal parameters ($l^*$ = 2, m = 2, Δr = 0.5, $q_0$ = 0.1 N/m, $x_0$ = 0.5L, c = L, $K_G$ = 0.01, $C_D$ = 5, $N^*$ = 0.001).

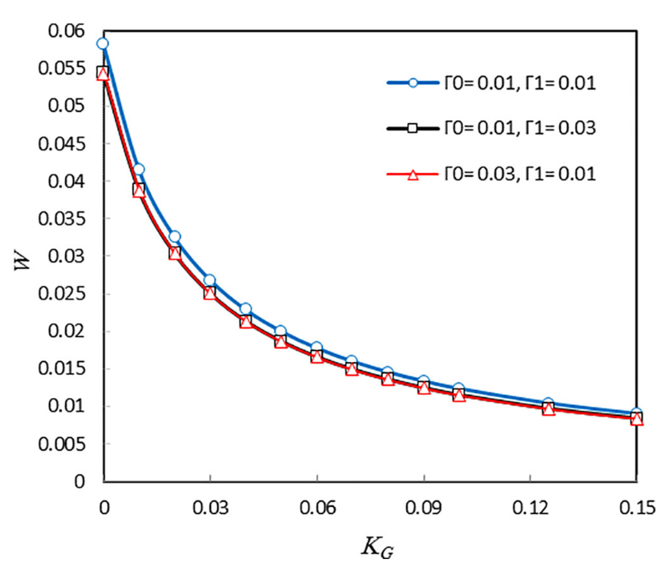


**Fig. 5b.** Shear modulus versus higher and lower-order nonlocal parameters ($l^*$ = 2, m = 2, Δr = 0.5, $q_0$ = 0.1 N/m, $x_0$ = 0.5L, c = L, $K_W$ = 0.01, $C_D$ = 5, $N^*$ = 0.001).

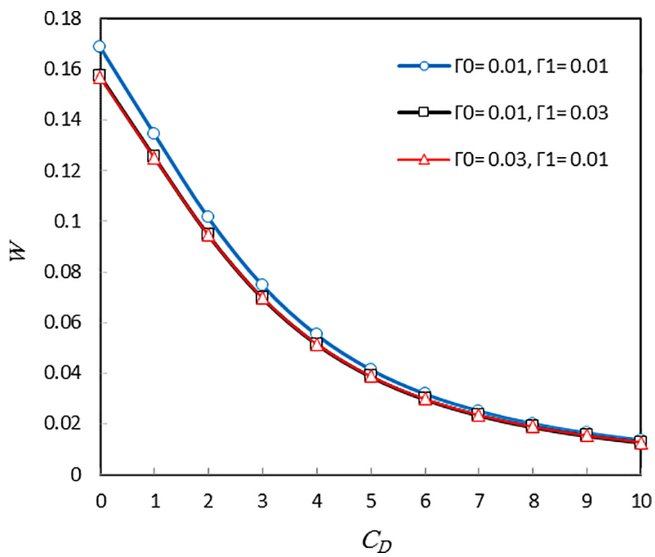


**Fig. 5c.** Viscous damper versus higher and lower-order nonlocal parameters ($l^* = 2$, $m = 2$, $\Delta r = 0.5$, $q_0 = 0.1$ N/m, $x_0 = 0.5L$, $c = L$, $K_W = 0.01$, $K_G = 0.01$, $N^* = 0.001$).

finally in large values of the shear modulus, the dynamic deflections obtained from various nonlocal conditions could be matched together. The influences of damping parameter on the results are studied in Fig. 5c. Naturally, in light of the vibrational analysis, the viscous parameter had more influence on the outcomes and that is in contrast to other foundation factors. It is noteworthy that by growing the value of the damper, the results of several cases are becoming closer to each other's. Indeed, it can be seen that large quantities of the foundation led to very small deflections, the effects of the higher-order nonlocal parameter are diminished and the use of lower-order strain gradient theory is enough in order to analyze the nanobeam under dynamic loads.

## 5. Conclusions

This article aimed to investigate the damped forced vibration of single-walled carbon nanotubes (SWCNTs) placing on a viscoelastic foundation embedded in the thermal environment, subjected to transverse harmonic dynamic loads. To achieve this aim, a novel first-order shear deformation beam theory combining with nonlocal strain gradient theory was formulated to derive the governing equations of motion. The influences of nanoscale were evaluated by the help of higher-order nonlocal strain gradient theory. Furthermore, the Navier's technique was used to calculate the numerical results. According to the numerical results of the present study, some notable points could be expressed as follows:

- Decreasing the stiffness of the nanobeam which originated from increasing values of nonlocal parameter, the effects of abating resonant vibration would be increased in physical structures of the nanobeam.
- Increasing temperature would increase the difference in the results of the higher and lower-order nonlocal cases.
- The larger values the deflections approach, the more significant the effects of the higher-order nonlocal parameter; and for the smaller values of deflections, there could be no requirement to use the higher-order nonlocal strain gradient theory.

## References


[1] M. Pacios Pujadó, Carbon Nanotubes as Platforms for Biosensors with Electrochemical and Electronic Transduction, Springer, Heidelberg, 2012. 10.1007/978-3-642-31421-6.
[2] F. Liu, R.M. Wagterveld, B. Gebben, M.J. Otto, P.M. Biesheuvel, H.V.M. Hamelers, Carbon nanotube yarns as strong flexible conductive capacitive electrodes, Colloids Interface Sci. Commun. 3 (2014) 9–12.
[3] Ch.B. Parker, A.S. Raut, B. Brown, B.R. Stoner, J.T. Glass, Three-dimensional arrays of graphenated carbon nanotubes, J. Mater. Res. 27 (2012) 1046–1053, https://doi.org/10.1557/jmr.2012.43.
[4] S. Iijima, Helical microtubules of graphitic carbon, Nature 354 (1991) 56–58.
[5] M.-F. Yu, O. Lourie, M.J. Dyer, K. Moloni, T.F. Kelly, R.S. Ruoff, Strength and breaking mechanism of multiwalled carbon nanotubes under tensile load, Science 287 (2000) 637–640.
[6] E. Pop, D. Mann, Q. Wang, K. Goodson, H. Dai, Thermal conductance of an individual single-wall carbon nanotube above room temperature, Nano Letters 6 (2005) 96–100.
[7] S. Sinha, S. Barjami, G. Iannacchione, A. Schwab, G. Muench, Off-axis thermal properties of carbon nanotube films, J. Nanoparticle Res. 7 (2005) 651–657.
[8] K.K. Koziol, D. Janas, E. Brown, L. Hao, Thermal properties of continuously spun carbon nanotube fibres, Physica E: Low-Dimensional Syst. Nanostruct. 88 (2017) 104–108.
[9] J.W. Mintmire, B.I. Dunlap, C.T. White, Are fullerene tubules metallic?, Phys Rev. Lett. 68 (1992) 631–634.
[10] X. Lu, Z. Chen, Curved Pi-Conjugation, aromaticity, and the related chemistry of small fullerenes (C60) and single-walled carbon nanotubes, Chem. Rev. 105 (2005) 3643–3696.
[11] T.A. Hilder, J.M. Hill, Modeling the loading and unloading of drugs into nanotubes, Small 5 (2009) 300–308.
[12] G. Pastorin, Crucial functionalizations of carbon nanotubes for improved drug delivery: a valuable option?, Pharmaceutical Res 26 (2009) 746–769.
[13] A.A. Bhirde, V. Patel, J. Gavard, G. Zhang, A.A. Sousa, A. Masedunskas, R.D. Leapman, R. Weigert, J.S. Gutkind, J.F. Rusling, Targeted killing of cancer cells in vivo and in vitro with EGF-directed carbon nanotube-based drug delivery, ACS Nano 3 (2009) 307–316.
[14] M. Malikan, M. Jabbarzadeh, Sh. Dastjerdi, Non-linear Static stability of bi-layer carbon nanosheets resting on an elastic matrix under various types of in-plane shearing loads in thermo-elasticity using nonlocal continuum, Microsyst. Technol. 23 (2017) 2973–2991.
[15] M. Malikan, Buckling analysis of a micro composite plate with nano coating based on the modified couple stress theory, J. Appl. Comput. Mech. 4 (2018) 1–15.
[16] M. Malikan, Analytical predictions for the buckling of a nanoplate subjected to nonuniform compression based on the four-variable plate theory, J. Appl. Comput. Mech. 3 (2017) 218–228.
[17] C. Feng, S. Kitipornchai, J. Yang, Nonlinear free vibration of functionally graded polymer composite beams reinforced with graphene nanoplatelets (GPLs), Eng. Struct. 140 (2017) 110–119.
[18] R. Ansari, R. Gholami, M. Faghih Shojaei, V. Mohammadi, M.A. Darabi, Coupled longitudinal-transverse-rotational free vibration of post-buckled functionally graded first-order shear deformable micro- and nano-beams based on the Mindlin's strain gradient theory, Appl. Math. Model. 40 (2016) 9872–9891.
[19] H.L. Dai, S. Ceballes, A. Abdelkefi, Y.Z. Hong, L. Wang, Exact modes for post-buckling characteristics of nonlocal nanobeams in a longitudinal magnetic field, Appl. Math. Modell. 55 (2017) 758–775.
[20] J. Jiang, L. Wang, Analytical solutions for thermal vibration of nanobeams with elastic boundary conditions, Acta Mechanica Solida Sinica 30 (2017) 474–483.
[21] L.L. Ke, Y. Xiang, J. Yang, S. Kitipornchai, Nonlinear free vibration of embedded double-walled carbon nanotubes based on nonlocal Timoshenko beam theory, Comput. Mater. Sci. 47 (2009) 409–417.
[22] L. Li, Y. Hu, buckling analysis of size-dependent nonlinear beams based on a nonlocal strain gradient theory, Int. J. Eng. Sci. 97 (2015) 84–94.
[23] L. Lu, X. Guo, J. Zhao, Size-dependent vibration analysis of nanobeams based on the nonlocal strain gradient theory, Int. J. Eng. Sci. 116 (2017) 12–24.
[24] H.-S. Shen, X.-Q. He, D.-Q. Yang, Vibration of thermally postbuckled carbon nanotube-reinforced composite beams resting on elastic foundations, Int. J. Non-Linear Mech. 91 (2017) 69–75.
[25] F. Mehralian, Y. Tadi Beni, M. Karimi Zeverdejani, Nonlocal strain gradient theory calibration using molecular dynamics simulation based on small scale vibration of nanotubes, Physica B: Cond. Matter 514 (2017) 61–69.
[26] Y.-Z. Wang, Y.-S. Wang, L.-L. Ke, Nonlinear vibration of carbon nanotube embedded in viscous elastic matrix under parametric excitation by nonlocal continuum theory, Physica E: Low-Dimensional Syst. Nanostruct. 83 (2016) 195–200.
[27] V.K. Chaudhari, A. Lal, Nonlinear free vibration analysis of elastically supported nanotube reinforced composite beam in thermal environment, Procedia Eng. 144 (2016) 928–935.
[28] F. Kheibari, Y.T. Beni, Size dependent electro-mechanical vibration of single-walled piezoelectric nanotubes using thin shell model, Mater. Design 114 (2017) 572–583.
[29] A. Ghorbani Shenas, P. Malekzadeh, S. Ziaee, Vibration analysis of pre-twisted functionally graded carbon nanotube reinforced composite beams in thermal environment, Compos. Struct. 162 (2017) 325–340.
[30] J. Jiang, L. Wang, Y. Zhang, Vibration of single-walled carbon nanotubes with elastic boundary conditions, Int. J. Mech. Sci. 122 (2017) 156–166.
[31] T.-P. Chang, Nonlinear vibration of single-walled carbon nanotubes with nonlinear damping and random material properties under magnetic field, Compos. Part B 114 (2017) 69–79.

[32] J. Jiang, L. Wang, Timoshenko beam model for vibrational analysis of double-walled carbon nanotubes bridged on substrate, Curr. Appl. Phys. 17 (2017) 1670–1690.
[33] G.-L. She, Y.-R. Ren, F.-G. Yuan, W.-Sh. Xiao, On vibrations of porous nanotubes, Int. J. Eng. Sci. 125 (2018) 23–35.
[34] S. Kamarian, M. Salim, R. Dimitri, F. Tornabene, Free vibration analysis of conical shells reinforced with agglomerated carbon nanotubes, Int. J. Mech. Sci. 108–109 (2016) 157–165.
[35] F. Tornabene, N. Fantuzzi, M. Bacciocchi, Free vibrations of free-form doubly-curved shells made of functionally graded materials using higher-order equivalent single layer theories, Compos. Part B-Eng. 67 (2014) 490–509.
[36] F. Tornabene, N. Fantuzzi, M. Bacciocchi, E. Viola, Effect of agglomeration on the natural frequencies of functionally graded carbon nanotube-reinforced laminated composite doubly-curved shells, Compos. Part B-Eng. 89 (2016) 187–218.
[37] D. Banić, M. Bacciocchi, F. Tornabene, A.J.M. Ferreira, Influence of Winkler-Pasternak foundation on the vibrational behavior of plates and shells reinforced by agglomerated carbon nanotubes, Appl. Sci. 7 (2017) 1228.
[38] N. Fantuzzi, F. Tornabene, M. Bacciocchi, R. Dimitri, Free vibration analysis of arbitrarily shaped Functionally Graded Carbon Nanotube-reinforced plates, Compos. Part B-Eng. 115 (2017) 384–408.
[39] M. Nejati, A. Asanjarani, R. Dimitri, F. Tornabene, Static and free vibration analysis of functionally graded conical shells reinforced by carbon nanotubes, Int. J. Mech. Sci. 130 (2017) 383–398.
[40] M. Nejati, R. Dimitri, F. Tornabene, Y.M. Hossein, Thermal buckling of nanocomposite stiffened cylindrical shells reinforced by functionally graded wavy carbon nano-tubes with temperature-dependent properties, Appl. Sci. 7 (2017) 1223.
[41] F. Tornabene, N. Fantuzzi, M. Bacciocchi, Linear static response of nanocomposite plates and shells reinforced by agglomerated carbon nanotubes, Compos. Part B-Eng. 115 (2017) 449–476.
[42] F. Tornabene, M. Bacciocchi, N. Fantuzzi, J. N. Reddy, Multiscale approach for three-phase CNT/Polymer/Fiber laminated nanocomposite structures, Polymer Composites, In Press, DOI: 10.1002/pc.24520.
[43] M. Malikan, Electro-mechanical shear buckling of piezoelectric nanoplate using modified couple stress theory based on simplified first order shear deformation theory, Appl. Math. Model. 48 (2017) 196–207.
[44] R.P. Shimpi, Refined plate theory and its variants, AIAA J. 40 (2002) 137–146.
[45] M. Malikan, Temperature influences on shear stability a nanosize plate with piezoelectricity effect, Multidiscipline Model. Mater. Struct. 14 (2018) 125–142.
[46] M. Malikan, M.N. Sadraee Far, Differential quadrature method for dynamic buckling of graphene sheet coupled by a viscoelastic medium using neperian frequency based on nonlocal elasticity theory, J. Appl. Comput. Mech. 4 (2018) 147–160, https://doi.org/10.22055/JACM.2017.22661.1138.
[47] C.W. Lim, G. Zhang, J.N. Reddy, A Higher-order nonlocal elasticity and strain gradient theory and Its Applications in wave propagation, J. Mech. Phys. Solids 78 (2015) 298–313.
[48] M.S. Nematollahi, H. Mohammadi, M.A. Nematollahi, Thermal vibration analysis of nanoplates based on the higher-order nonlocal strain gradient theory by an analytical approach, Superlattices Microstruct. 111 (2017) 944–959.
[49] M.R. Barati, A. Zenkour, A general bi-Helmholtz nonlocal strain-gradient elasticity for wave propagation in nanoporous graded double-nanobeam systems on elastic substrate, Compos. Struct. 168 (2017) 885–892.
[50] M. Malikan, V.B. Nguyen, Buckling analysis of piezo-magnetoelectric nanoplates in hygrothermal environment based on a novel one variable plate theory combining with higher-order nonlocal strain gradient theory, Physica E: Low-Dimensional Syst. Nanostruct. 102 (2018) 8–28.
[51] M.R. Barati, H. Shahverdi, A general nonlocal stress-strain gradient theory for forced vibration analysis of heterogeneous nanoporous plates, Eur. J. Mech./A Solids 67 (2018) 215–230.
[52] E. Ghavanloo, S.A. Fazelzadeh, Vibration characteristics of single-walled carbon nanotubes based on an anisotropic elastic shell model including chirality effect, Appl. Math. Model. 36 (2012) 4988–5000.
[53] D.H. Robertson, D.W. Brenner, J.W. Mintmire, Energetics of nanoscale graphitic tubules, Phys. Rev. B 45 (1992) 12592.
[54] A. Benzair, A. Tounsi, A. Besseghier, H. Heireche, N. Moulay, L. Boumia, The thermal effect on vibration of single-walled carbon nanotubes using nonlocal Timoshenko beam theory, J. Phys. D: Appl. Phys. 41 (2008) 2254041–2254110.
[55] T. Murmu, S. Adhikari, Nonlocal transverse vibration of double-nanobeam-systems, J. Appl. Phys. 108 (2010) 083514.
[56] P. Ponnusamy, A. Amuthalakshmi, Influence of thermal and magnetic field on vibration of double walled carbon nanotubes using nonlocal Timoshenko beam theory, Procedia Mater. Sci. 10 (2015) 243–253.